Layered and Hexagonal Aluminosilicate−Hexadecylamine Mesostructures: Solid State Transformation and Ionic Conductivity

Sang Kyeong Yun and Joachim Maier*

Max-Planck-Institut für Festkörperforschung, Heisenbergstrasse 1, 70569 Stuttgart, Germany

Received March 12, 1998

Inorganic−organic hybrids of the aluminosilicate−hexadecylamine mesostructures (AHM) have been prepared by a sol−gel reaction of tetraethyl orthosilicate (TEOS) and $Al(NO_3)_3 \cdot 9H_2O$ mixtures in the presence of hexadecylamine (HDA) and $LiNO_3$. At an HDA concentration of [HDA]/([Si] + [Al]) = 0.3, both lamellar and hexagonal AHM structures were obtained, depending on the degree of Al substitution and $LiNO_3$ addition. Our synthetic work illustrates that the inorganic ingredient ($LiNO_3$) as well as the sol−gel precursor ($Al(NO_3)_3$) plays a crucial role in the selective formation of the lamellar or hexagonal AHM. Without an Al or a Li source, products obtained by the same method were all found to have exclusively the hexagonal structure. Studies using XRD, DSC, high-resolution TEM, and selected area electron diffraction (SAED) verified that the prepared lamellar AHMs undergo (i) a reversible melting of the HDA intercalates at 60 °C and then (ii) an irreversible structural transformation to their hexagonal analogues at higher temperature. The temperature dependence of the ionic conductivity (σ) revealed a strong structural sensitivity. We discuss in more detail the conduction behavior of a $[Si_{17.1}Al_{1.00}O_{36.2}(Li_{0.47}H_{0.53})][HDA]_{21.0}$ product in its lamellar structure (exhibiting moderate conductivities of $\sim 10^{-7}$ S/cm below 50 °C), in its highly conductive HDA-melted metastable layered structure ($\sim 10^{-4}-10^{-3}$ S/cm in the region of 60−210 °C), and in its comparatively insulating hexagonal structure ($10^{-9}-10^{-8}$ S/cm between 130 and 260 °C).

Introduction

Silica-based mesoporous molecular sieves (M41S) have received considerable attention due to their unique structural features of well-defined pore systems.[1] Three mesostructures, the lamellar, hexagonal, and cubic, were derived by surfactant-templated sol−gel routes under controlled reaction conditions. Extensive efforts to study their applicability as catalysts,[2] ionic adsorbent materials,[3] and host materials for photosensitizers,[4] conducting polymers,[5] and nanoparticles[6] have been made using hexagonal and cubic M41S materials with uniform mesopores approximately 20−100 Å in diameter.

In contrast to the extensively studied hexagonal and cubic materials, the lamellar structure has not been explored with respect to any materials applications until now. Useful materials properties of the lamellar structure materials, however, are expected to be found by chemically modifying the interfacial region between the inorganic metal oxide layer and the organic templates. One possibility is to substitute Si atoms of the two-dimensional silica network with other metals such as Al, as a consequence of which a foreign chemical species (e.g., H^+, Li^+, or Na^+) can be introduced into the inorganic−organic interfacial region for electrostatic charge compensation.

In this study, aluminosilicate−hexadecylamine mesostructures (AHM) of the M41S-type materials have been prepared by a conventional sol−gel reaction of tetraethyl orthosilicate (TEOS) and $Al(NO_3)_3 \cdot 9H_2O$ mixtures in the presence of hexadecylamine (HDA). At a surfactant concentration of [HDA]/([Si] + [Al]) = 0.3 the final structure of obtained AHM products, hexagonal or lamellar, was found to be governed by the degree of Al substitution and $LiNO_3$ addition. We also observed that the inorganic ingredient ($LiNO_3$) as well as the sol−gel precursor ($Al(NO_3)_3$) plays a crucial role in the selective formation of the lamellar or hexagonal AHM. In addition, XRD, DSC, high-resolution TEM, and selected area electron diffraction (SAED) studies indicated an irreversible thermal structural transformation of the prepared lamellar mesostructures to their hexagonal analogues, which enabled us to compare their ionic conductivities. Here we report on the significant structural dependence of the ionic conductivity (σ), amounting to a difference of more than 4 orders of magnitude, during the course of the solid-state phase changes. We present the case of an AHM product $[Si_{17.1}Al_{1.00}O_{36.2}(Li_{0.47}H_{0.53})][HDA]_{21.0}$ in its lamellar, HDA-melted metastable layered and hexagonal structures. Observed ionic conductivities are attributed to ion hopping (mostly proton and presumably lithium ion) through the aluminosilicate and HDA interfaces of the AHM frameworks.

* To whom correspondence should be addressed.

(1) (a) Kresge, C. T.; Leonowicz, M. E.; Roth, W. J.; Vartuli, J. C.; Beck, J. S. *Nature* **1992**, *359*, 710−712. (b) Beck, J. S.; Vartuli, J. C.; Roth, W. J.; Leonowicz, M. E.; Kresge, C. T.; Schmitt, K. D.; Chu, C. T−W.; Olson, D. H.; Sheppard, E. W.; McCullen, S. B.; Higgins, J. B.; Schlenker, J. L. *J. Am. Chem. Soc.* **1992**, *114*, 10834−10843.

(2) (a) Tanev, P. T.; Chibwe, M.; Pinnavaia, T. J. *Nature* **1994**, *368*, 321−323. (b) Maschmeyer, T.; Rey, F.; Sankar, G.; Thomas, J. M. *Nature* **1995**, *378*, 159−162. (c) Schüth, F. *Ber. Bunsen-Ges. Phys. Chem.* **1995**, *99*, 1306−1315. (d) Kloetstra, K. R.; van Bekkum, H. *J. Chem. Soc., Chem. Commun.* **1995**, 1005−1006. (e) Corma, A.; Iglesias, M.; Sánchez, F. *J. Chem. Soc., Chem. Commun.* **1995**, 1635−1636. (f) Zhang, W.; Pinnavaia, T. J. *Catal. Lett.* **1996**, *38*, 261−265.

(3) Feng, X.; Fryxell, G. E.; Wang, L.-Q.; Kim, A. Y.; Liu, J.; Kemner, K. M. *Science* **1997**, *276*, 923−926.

(4) Cano, M. L.; Corma, A.; Fornés, V.; Garcìa, H.; Miranda, M. A.; Baerlocher, C.; Lengauer, C. *J. Am. Chem. Soc.* **1996**, *118*, 11006−11013.

(5) Wu, C.-G.; Bein, T. *Science* **1994**, *264*, 1757−1759.

(6) (a) Chomski, E.; Dag, Ö.; Kuperman, A.; Coombs, N.; Ozin, G. A. *Chem. Vap. Deposition* **1996**, *2*, 8−13. (b) Abe, T.; Tachibana, Y.; Uematsu, T.; Iwamoto, M. *J. Chem. Soc., Chem. Commun.* **1995**, 1617−1618.

10.1021/ic980276w CCC: $18.00
Published on Web 02/08/1999

Experimental Section

Materials. Tetraethyl orthosilicate (Aldrich, 98%), $Al(NO_3)_3 \cdot 9H_2O$ (Merck, >98.5%), hexadecylamine (Alfa, 98%), $LiNO_3$ (Merck, Suprapure), and ethanol (Carl Roth, 99.8%) were used as received without further treatment. Doubly distilled water was used for the handling of all aqueous solutions.

Synthesis. Typically, 72.5 mmol of HDA was dissolved in an ethanol (100 mL)−water (80 mL) mixture at 50 °C. Solid $LiNO_3$ (12.1 mmol) was then added to the surfactant solution. A mixture of TEOS (230 mmol) and $Al(NO_3)_3 \cdot 9H_2O$ (12.1 mmol), homogenized in 50 mL of ethanol under nitrogen at room temperature, was then delivered into the clear surfactant solution having mole fraction [HDA]/([Si] + [Al]) = 0.3 with stirring at 50 °C. A glass cover was placed on the reaction vessel. White precipitates formed within several minutes and were aged at 50 °C for 30 h. A small opening in the reaction container allowed slow evaporation of the alcohol, which was present and produced by the hydrolysis of TEOS. The resulting product, having a [Si]:[Al]:[Li] ratio of 19:1:1, was filtered, washed with ~1.5 L water under suction, and finally dried in air at ambient temperature. The product obtained, an aluminosilicate−HDA mesostructure, is hereafter denoted as AHM-X. Two more syntheses, with [Si]:[Al]:[Li] ratios of 19:1:5 and 17:3:3, were carried out using the same reaction procedure and treatment, the products of which being designated as AHM-Y and AHM-Z, respectively. Elemental analysis revealed the product compositions of the $[Si_xAl_{1.00}O_{2(x+1)}(Li_{1-z}H_z)][HDA]_n$ stoichiometry: AHM-X, $x = 18.1$, $z = 0.94$, $n = 6.56$; AHM-Y, $x = 17.1$, $z = 0.53$, $n = 21.0$; AHM-Z, $x = 6.03$, $z = 0.99$, $n = 17.7$.

In other sets of syntheses (i−iii), we prepared by the same method (i) a silica−HDA (with neither Al source nor $LiNO_3$), (ii) an aluminosilicate−HDA with a 19:1 ratio of [Si] to [Al] (without $LiNO_3$), and (iii) two silica−HDA products with [Si]:[Li] ratios of 18:2 and 16:4 (without an Al source). Products from these three sets all showed XRD patterns characteristic of the hexagonal mesostructure (see below).

Characterization and Conductivity Measurements. Powder XRD patterns were taken at room temperature using a Philips PW3710 diffractometer with Cu Kα *x*-radiation. Data were collected every 0.01° from $2\theta = 1.5-40.0°$. Scanning electron microscopy (SEM) and high-resolution transmission electron microscopy (HRTEM) studies were performed with a Leica Stereoscan 420 system and a Philips CM 200, respectively. Samples were prepared for TEM by dipping carbon-coated copper grids into a suspension in ethanol of the powdered sample. TEM images were taken at an acceleration voltage of 200 kV. SAED measurements were taken under the same 200 kV condition. Differential scanning calorimetry (DSC) profiles were obtained with a Setaram DSC 121 system at temperatures ranging from room temperature to 700 °C (1 °C/min) under nitrogen flow.

Elemental analyses of Si, Al, Li, and N were done by inductively coupled plasma (ICP) emission spectroscopy and by the thermal extraction method. The amounts of the framework oxygen and hydrogen atoms are calculated on the basis of the assumptions that the elements are in their typical oxidation state and that the charge deficiency created by substituting Al^{3+} for Si^{4+} is compensated by Li^+ or H^+. The amount of HDA was derived from the nitrogen analysis.

Ionic conductivity was measured by impedance analysis from room temperature to 270 °C using a Solartron 1260 impedance analyzer. The applied signal amplitude was 80 mV in the frequency range 1.0 Hz to 30 MHz. Room temperature curing platinum paste (from Demetron GmbH) was applied to both sides of a disk sample (0.1 cm in thickness and 0.8 cm in diameter) and pressed at 80 kN, to provide better contacts to the platinum electrodes. Data were taken after a 30 min period at each temperature (±0.5 °C) under dry Ar flow, when values had reached a constant reading.

Results and Discussion

Synthesis and Characterization. In our synthesis, incorporation of Al cations into the silica framework of M41S-type materials has been achieved by a conventional sol−gel route using TEOS and $Al(NO_3)_3 \cdot 9H_2O$ in the presence of HDA. Lithium ion as $LiNO_3$ was added for charge compensation of the Si substitution by Al.

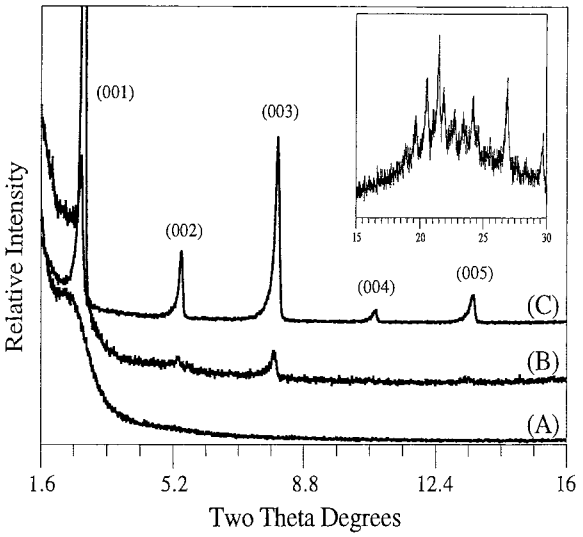

Figure 1. Powder XRD patterns of (A) AHM-X, (B) AHM-Y, and (C) AHM-Z. (00*l*) reflections are indexed on the basis of the hexagonal structure of the M41S-type material. Both the AHM-Y and -Z products exhibited well-resolved XRD reflections due to the interlayer HDA packing at the 2θ range shown for AHM-Y in the inset.

The AHM-X product, prepared with a [Si]:[Al]:[Li] molar ratio of 19:1:1 at [HDA]/([Si] + [Al]) = 0.3, exhibited an XRD pattern characteristic of the hexagonal structure (Figure 1A). That is, $d_{001} = 38.7$ Å appears as a broad shoulder, as in other hexagonal M41S materials prepared under similar conditions.[7] Quite unexpectedly, the same reaction but with a [Si]:[Al]:[Li] ratio of 19:1:5 (i.e., 5× excess of $LiNO_3$) resulted in a lamellar structure of the AHM-Y product. Powder XRD revealed several (00*l*) reflections with a basal spacing of 32.6 Å for the AHM-Y sample (Figure 1B). However, the same reaction using no $LiNO_3$ produced a hexagonal structure identical to AHM-X (see Experimental Section). These observations demonstrate the important role of the inorganic ingredient (here $LiNO_3$) in the structural development, hexagonal or lamellar, of the M41S-type inorganic/organic mesostructures.

Kumar and co-workers[15] have recently reported on the structure-directing role of small inorganic promoters, such as MX ($M = Na^+$ or K^+; $X = NO_3^-$, ClO_4^-, or SO_4^{2-}), in the formation of zeolite-type silicate materials that have been organic amine templated. According to Kumar et al., the presence of such promoter ions greatly polarizes the hydrophobic hydration spheres formed around oligomeric silicate units and

(7) Tanev, P. T.; Pinnavaia, T. J. *Science* **1995**, *267*, 865−867.
(8) Huo, Q.; Margolese, D. I.; Ciesla, U.; Feng, P.; Gier, T. E.; Sieger, P.; Leon, R.; Petroff, P. M.; Schüth, F.; Stucky, G. D. *Nature* **1994**, *368*, 317−321.
(9) Antonelli, D. M.; Ying, J. Y. *Chem. Mater.* **1996**, *8*, 874−881.
(10) Bagshaw, S. A.; Prouzet, E.; Pinnavaia, T. J. *Science* **1995**, *269*, 1242−1244.
(11) Schacht, S.; Huo, Q.; Voigt-Martin, I. G.; Stucky, G. D.; Schüth, F. *Science* **1996**, *273*, 768−771.
(12) Huo, Q.; Leon, R.; Petroff, P. M.; Stucky, G. D. *Science* **1995**, *268*, 1324−1327.
(13) Firouzi, A.; Kumar, D.; Bull, L. M.; Besier, T.; Sieger, P.; Huo, Q.; Walker, S. A.; Zasadzinski, J. A.; Glinka, C.; Nicol, J.; Margolese, D.; Stucky, G. D.; Chmelka, B. F. *Science* **1995**, *267*, 1138−1143.
(14) (a) Oliver, S.; Kuperman, A.; Coombs, N.; Lough, A.; Ozin, G. A. *Nature* **1995** *378*, 47−50. (b) Khushalani, D.; Kuperman, A.; Ozin, G. A.; Tanaka, K.; Garces, J.; Olken, M. M.; Coombs, N. *Adv. Mater.* **1995**, *7*, 842−846.
(15) Kumar, R.; Bhaumik, A.; Ahedi, R. K.; Ganapathy, S. *Nature* **1996**, *381*, 298−300.

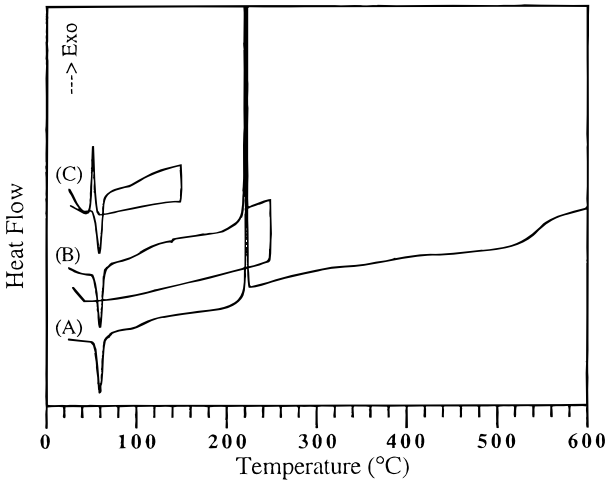

Figure 2. DSC profiles of the AHM-Y sample during the heating−cooling cycles: (A) room temperature (RT) to 700 °C; (B) RT to 250 °C, then back to RT; (C) RT to 150 °C, and back to RT. The endotherm at 60 °C and the exotherm at 220 °C in A correspond to the melting of interlayer HDAs and the transition to the hexagonal analogue, respectively (see text).

the alkyl groups of the organic structure-directing agent. Though no clear explanation is available at the moment, our lamellar and hexagonal AHM products also seem to be greatly influenced by different modes of counterion binding and interaction with the surfactant headgroups, of which the importance and phase-directing role have been reported for other surfactant systems.[16]

Interestingly, by increasing the degree of Al substitution, while keeping constant the Al:Li ratio ([Si]:[Al]:[Li] ratio of 17:3:3), we obtained a crystalline lamellar structure of the AHM-Z product as indicated by its XRD patterns (Figure 1C). In addition to the 5 orders of (00*l*) reflections, both the AHM-Y and -Z products exhibited additional X-ray reflections at higher angles of $2\theta = 18-36°$, indicating the presence of HDA hydrocarbon chain packing between the aluminosilicate layers.[17]

In an attempt to further understand the structure-directing factors, we performed other sets of preparations without any Al source (see Experimental Section). Under the same reaction condition as employed for the preparation of the above AHM series, two different reactant ratios of [Si]:[Li] (18:2 and 16:4) were adapted for the synthesis. In a separate experiment the purely siliceous product, using neither the Al nor the Li source, was also prepared by the same procedure. All three products were found to have the hexagonal structure, according to their XRD patterns. These results imply that the combined effect of the inorganic ingredient (here $LiNO_3$) and the sol−gel precursor (here $Al(NO_3)_3$) plays a crucial role in the selective formation of the lamellar or hexagonal M41S-type structure.

Structural Transformation. The DSC of the lamellar AHM-Y product exhibited a reversible endotherm at 60 °C, followed by an irreversible endotherm at ∼95 °C (Figure 2). The former is attributed to the melting of interlayer HDA templates,[18] while the latter is due to water desorption. A room temperature XRD pattern taken after a 10 h heating at 100 °C verified that no structural change had occurred upon the melting and resolidification (at 52 °C) process of the interlayer HDAs, corresponding to the thermal process in Figure 2C. On the other hand, the hexagonal AHM-X product did not show any melting behavior of the interlayer HDAs during the same DSC running; instead the surfactant decomposed at about 500 °C as in other reported hexagonal M41S materials.[1,2,7−13]

A sharp irreversible exotherm at 220 °C was observed upon further heating of the AHM-Y sample, as shown in Figure 2A,B. A room temperature XRD pattern taken after a 10 h thermal treatment at 240 °C indicated a hexagonal structure. The increased interlayer surfactant association and concomitant structural reorganization are believed to be responsible for the observed transformation of the lamellar AHM-Y to its hexagonal analogue.[17,19] The lamellar AHM-Z product also exhibited an endotherm of the interlayer HDA melting (at 60 °C) and an irreversible exotherm (at 165 °C) due to the transformation into its hexagonal structure, examined by DSC and XRD studies.

High-resolution TEM combined with SAED studies afforded an in situ monitoring of the solid state transformation from the lamellar to the hexagonal structure. Shown in Figure 3 are the TEM and SAED images of a selected AHM-Y microcrystal taken at three steps during the course of its transformation under a 200 kV electron beam. The lattice reflection with its two-dimensional SAED pattern (Figure 3A) was found to experience a lattice distortion along the axis bisecting the crystal (Figure 3B), upon about 10 min exposure to the e-beam under vacuum. Also, SAED indicates that some kind of structural changes occur at this stage. On further exposure, the crystal became featureless but with a unidimensional SAED (Figure 3C). These TEM and SAED changes indicate that the two-dimensional lamellar structure is rearranged into a unidimensional hexagonal M41S-type structure.

Until now there were three ways of transforming lamellar M41S-type materials into hexagonal analogues, all relying on solution routes. Intercalation-assisted[20] or solvent extraction-assisted[21] removal of surfactant templates followed by a high-temperature (at ∼500 °C) calcination process has been claimed to effectively condense 2-dimensional silicates into the hexagonal structure of M41S-type materials. A postsynthetic hydrothermal treatment in water is also an effective route to achieve the same lamellar to hexagonal structure transition.[17] Different from these approaches, our observation presents a solid state route of the thermal restructuring of the lamellar M41S-type materials to the hexagonal structure. That is, as-synthesized solid products of our lamellar AHM materials may be thermally treated to melt the interlayer HDA surfactants at ∼60 °C, which eventually gives rise to the structural transformation to a hexagonal structure at higher temperatures.

Ionic Conductivity. DSC showed the absence of a separate $LiNO_3$ phase in all AHM products. Hence, all incorporated lithium ions appear to be ionically bonded to the oxygen framework of the aluminosilicate. These lithium ions may then be able to hop through the interfacial region between the metal oxide backbone and the amine nitrogen network. According to the elemental analysis, however, our AHM products contain an appreciable amount of protons as well as lithium ions compen-

(16) Sein, A.; Engberts, J. B. F. N. *Langmuir* **1995**, *11*, 455−465.
(17) Huo, Q.; Margolese, D. I.; Stucky, G. D. *Chem. Mater.* **1996**, *8*, 1147−1160.
(18) The DSC profile of the neat hexadecylamine (Alfa, 98%) used in the present study showed its melting point at 48 °C. The AHM-Y sample retained its powderous form all through the thermal treatment, regardless of the melting and solidification of interlayer HDA templates.
(19) Monnier, A.; Schüth, F.; Huo, Q.; Kumar, D.; Margolese, D.; Maxwell, R. S.; Stucky, G. D.; Krishnamurty, M.; Petroff, P.; Firouzi, A.; Janicke, M.; Chmelka, B. F. *Science* **1993**, *261*, 1299−1303.
(20) (a) Inagaki, S.; Fukushima, Y.; Kuroda, K. *J. Chem. Soc., Chem. Commun*. **1993**, 680−682. (b) O'Brien, S.; Francis, R. J.; Price, S. J.; O'Hare, D.; Clark, S. M.; Okazaki, N.; Kuroda, K. *J. Chem. Soc., Chem. Commun*. **1995**, 2423−2424.
(21) Ulagappan, N.; Battaram, N.; Raju, V. N.; Rao, C. N. R. *Chem. Commun.* **1996**, 2243−2244.

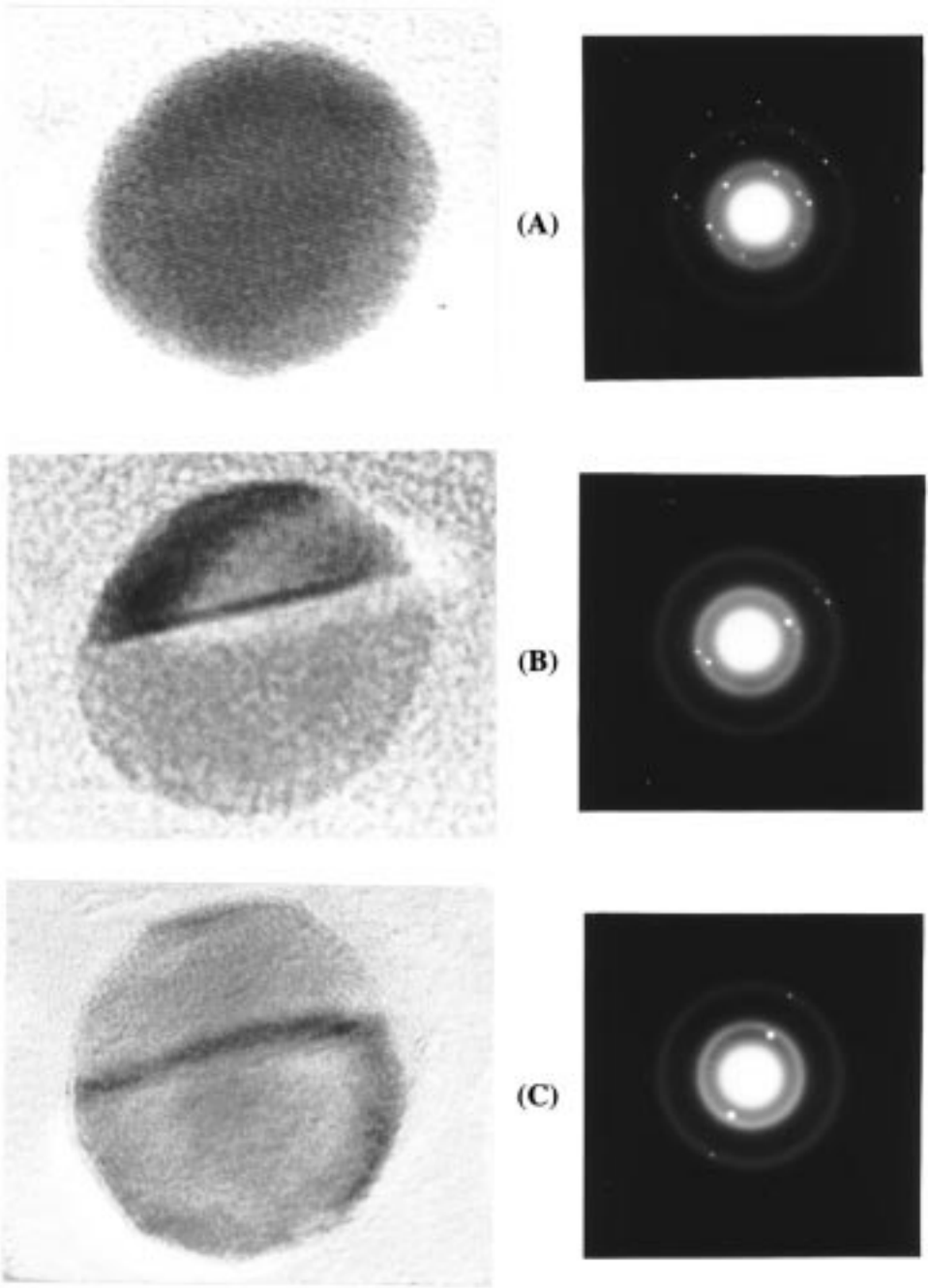

Figure 3. Changes of the high-resolution TEM and SAED images of the AHM-Y microcrystal upon exposure to electron beam irradiation (200 kV) under vacuum: (A) 0 min; (B) 10 min; (C) 45 min. About 2.7 Å spacings of the (*hk*0) lattice reflections are visible in A and B.

sating the charge loss due to the partial Al substitution among the framework Si (see Experimental Section). Therefore, the conductivity observed for the prepared AHM products probably stems from protons and/or lithium ions.

We studied the temperature and structural dependence of the ionic conductivity of our AHM materials. Since both AHM-Y and -Z behave similarly, we report on AHM-Y, which exhibits a wide temperature range in which the highly conducting phase is durable.[22] Figure 4 shows the temperature-dependent conduction behavior of the AHM-Y sample for the different structures existing in different temperature regimes. Conductivity measurements were carried out with four consecutive heating and cooling cycles: (i) room temperature to ~150 °C, (ii) ~150 °C to room temperature, (iii) 140 °C to ~260 °C, and (iv) ~260 °C to 140 °C.

Upon heating the AHM-Y sample (cycle i in Figure 4), ionic conductivities of less than 5.65×10^{-7} S/cm (at 50 °C) increased to 1.35×10^{-4} S/cm (at 60 °C) and 6.14×10^{-4} S/cm (at 152 °C). Differences in the conductivity observed in cooling back to room temperature (cycle ii in Figure 4) are attributed to a protonic contribution upon the thermal water desorption, as is usually encountered in sol−gel derived aluminosilicate materials.[23] Surprisingly, in the heating and cooling cycles an abrupt change of more than 3 orders of magnitude was apparant at ~50 °C, at which point the interlayer HDA starts to melt. This

(22) The highly conducting metastable layered structure was observed between 60 and 165 °C for the AHM-Z product.

(23) (a) Wang, B.; Szu, S.; Greenblatt, M. *Chem. Mater.* **1992**, *4*, 191−197. (b) Laby, L.; Klein, L. C.; Yan, J.; Greenblatt, M. *Solid State Ionics* **1995**, *81*, 217−224.

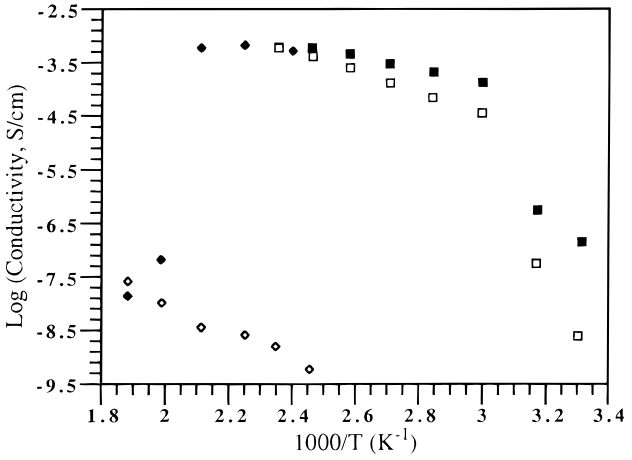

Figure 4. Temperature-dependent ionic conductivities of the AHM-Y sample. Measurements were carried out with four consecutive heating and cooling cycles using the same pellet: (i) room temperature (RT) to ~150 °C (■); (ii) ~150 °C to RT (□); (iii) 140 °C to ~260 °C (◆); (iv) ~260 °C to 140 °C (◇).

indicates that the ionic transport along the two-dimensional aluminosilicate−HDA interfaces is greatly facilitated by the melting of the interlayer HDA, as noted by the lower activation energy of 0.39 eV in the 60−150 °C range compared to 2.00 eV below 50 °C.

Upon reheating of the cooled sample (cycle iii in Figure 4), the conductivity reached a maximum of 6.69×10^{-4} S/cm at 172 °C, where the HDA-melted phase exists. It is worth noting that, compared with the reported lithium aluminosilicates[23] and the phyllosilicates of metal ion complexed poly(ethylene oxide) intercalates,[24] the AHM-Y sample shows higher ion conductivities, by up to 2 orders of magnitude, in the same temperature range. According to the literature,[23,24] the sol−gel derived lithium aluminosilicates exhibit ionic conductivity by the conventional hopping mechanism, while in the phyllosilicate composites the conduction occurs through the oxygen channel of intercalated poly(ethylene oxide). In the HDA-melted layered AHM-Y structure, the highly dynamic nature of the molten interlayer HDA and its association with the interfacial protons and lithium ions, which is not available in the hexagonal structure, would account for the enhanced ionic conductivity of the HDA-melted layered AHM-Y structure (see below).

Considerable decrease in the ion conductivity is then observed at temperatures above 230 °C and in the last cooling step (cycle iv in Figure 4), where AHM-Y exists as a hexagonal structure. The irreversible structure change resulted in a decrease of about 5 orders of magnitude in conductivity, for example, 6.69×10^{-4} S/cm (at 172 °C) vs 2.60×10^{-9} S/cm (at 171 °C) for the layered and hexagonal AHM-Y, respectively. Similar σ values of about 10^{-9} S/cm orders were also observed for the hexagonal AHM-X sample. It is also important to note that the AHM-Z product with almost no lithium ions exhibited only less than an order of magnitude decrease in conductivity compared to AHM-Y at 60−165 °C, where both products exist as the HDA-melted metastable layered structure. This is evidence that the observed conductivity stems from mainly protonic conduction. Since proton migration demands pronounced detachment and migration modes, the increase of the conductivity in the partially molten state is clearly expected.[25]

In an attempt to investigate the proposed anisotropic nature[26] of the observed ionic conductivity, no appreciable differences were found for the perpendicular and parallel directions of AHM-Y. SEM studies showed no preferential grain orientation either in the original powder mixture or in the pressed final sample. Consequently the impedance response is sampling domains of different orientations, and the anisotropy could not be measured.

Summary

We have presented a new sol−gel control for the selective formation of the lamellar and hexagonal structures of aluminosilicate−HDA mesostructures (AHM). The part of our study dealing with synthesis demonstrates the structure-directing roles of added inorganic ingredient ($LiNO_3$) and Al precursor ($Al(NO_3)_3$). Also reported is an irreversible solid state thermal transformation of the layered AHMs into their hexagonal analogues, verified by XRD, DSC, HRTEM, and SAED studies. We have demonstrated the temperature and structural dependence of the ionic conductivity of an AHM material during the course of its transformation. Differences of more than 4 orders of magnitude in conductivity have been found between three temperature ranges where lamellar, HDA-melted metastable layered and hexagonal AHM structures are distinguished. The highest conductivities (3.59×10^{-5} to 6.69×10^{-4} S/cm) are observed in the HDA-melted metastable layered structure of the AHM-Y product, most probably due to the highly dynamic interaction of the molten interlayer HDAs with the interfacial ions. In comparison, the hexagonal analogue with the same composition exhibited much lower ionic conductivities by about 5 orders of magnitude. The similar conductivity behavior of the two AHM-Y and -Z compounds with very different Li contents points toward a protonic conductivity. Nevertheless, the presence of the Li source is necessary to achieve the lamellar structure.

Acknowledgment. We thank Ms. M. Kelsch from the Max Planck Institute for Metal Research for technical assistance in performing HRTEM studies. S.K.Y is also thankful to the Max-Planck-Gesellschaft for a research scholarship.

IC980276W

(24) (a) Ruiz-Hitzky, E.; Aranda, P. *Adv. Mater.* **1990**, *2*, 545−547. (b) Aranda, P.; Ruiz-Hitzky, E. *Chem. Mater.* **1992**, *4*, 1395−1403. (c) Vaia, R. A.; Vasudevan, S.; Krawiec, W.; Scanlon, L. G.; Giannelis, E. P. *Adv. Mater.* **1995**, *7*, 154−156.

(25) Kreuer, K. D. *Solid State Ionics* **1997**, *97*, 1−15 and references therein.

(26) Aranda, P.; Ruiz-Hitzky, E. *Chem. Mater.* **1992**, *4*, 1395−1403.